Interference of Magnetic and Anisotropic Tensor Susceptibility Reflections in Resonant X-Ray Scattering of GdB_4

S. Ji,[1] C. Song,[1] J. Koo,[1] K.-B. Lee,[1,2] Y. J. Park,[1,2] J. Y. Kim,[2] J.-H. Park,[1] H. J. Shin,[2] J. S. Rhyee,[3] B. H. Oh,[3] and B. K. Cho[3]

[1]*eSSC and Department of Physics, Pohang University of Science and Technology, Pohang, 790-784, South Korea*
[2]*Pohang Accelerator Laboratory, Pohang University of Science and Technology, Pohang, 790-784, South Korea*
[3]*Center for Frontier Materials and Department of Materials Science and Engineering, K-JIST, Kwangju, 500-712, South Korea*

(Received 27 June 2003; published 16 December 2003)

Resonant x-ray scattering experiments at the Gd L_3 edge show interference between magnetic and anisotropic tensor susceptibility (ATS) reflections in GdB_4. Energy profiles obtained from the magnetic and ATS resonances exhibited $\sim$10 eV separation between the maximum resonance energies. The findings show that the Gd $5d$ band experienced hybridization giving rise to a significant split into isotropic lower energy band and distorted upper band states that account for the magnetic and ATS scattering, respectively.

DOI: 10.1103/PhysRevLett.91.257205 PACS numbers: 75.25.+z, 78.70.Ck

Resonant x-ray scattering (RXS) is becoming a prominent technique as an ideal probe of local environment and electronic structures. The RXS process involves electric multipole transitions by exciting a core electron of a corresponding absorption edge to an empty valence shell of intermediate state. Direct involvement of this valence orbital gives rise to an enhanced sensitivity to the target ion's magnetic moment and anisotropic charge distribution (anisotropy of x-ray susceptibility tensor) influenced by the net spin polarization and chemical bondings, respectively [1–6]. The net spin polarization at the valence shell enables the x-ray resonance exchange scattering. Distortion of the valence shell in a crystalline environment caused by a chemical bonding/hybridization or crystalline electric fields by surrounding ions leads to an anisotropic tensor of the x-ray susceptibility which reflects the symmetry of the chemical environment. The general reflection condition (systematic extinction of Bragg reflections from glide plane and screw axis symmetry operations) derived for an isotropic x-ray susceptibility is no longer fulfilled, thus, producing the so-called forbidden reflection [ATS (anisotropic tensor susceptibility) reflection].

Extensive use of the RXS was employed mainly for the investigation of cooperative orderings of electric orbital/quadrupole, or magnetic moments as well as more generic crystal symmetry related forbidden reflections such as the (0 0 6) reflection of Ge [6–10]. While the RXS has led to a spectacular progress unveiling microscopic properties of materials, capability of RXS as a spectroscopy probe has not been fully explored. Also, most of the experimental work has been limited by employing either magnetic sensitivity or ATS, separately. Although the combined anisotropy effects have been theoretically proposed [1,11], neither experimental consideration nor demonstrative evidence of combined anisotropies, such as magnetic and chemical, has been addressed until now.

In this Letter, we present an explicit evidence of interference between magnetic and ATS resonances in GdB_4 from the Gd L_3-edge RXS. Manipulation of the magnetic and ATS contribution to the interference scattering was realized with the azimuthal ψ rotation, $\vec{\psi} \parallel (\vec{Q} = \vec{k}_f - \vec{k}_i)$, as well as temperature variation and energy. Furthermore, comparison of the magnetic and ATS resonance energy profile suggests that intra- and interatomic mixing of the Gd $5d$ band lead to independent characters of spin polarization and anisotropic distortion of the $5d$ orbital. Most significantly, RXS energy profiles manifested electronic structures where distinction of the different states was achieved by satisfying the selection rules corresponding to each state.

GdB_4 crystallizes in a tetragonal structure ($P4/mbm$), and Gd ions are located at the $4g$ symmetry positions. Ground state physical property is characterized by an antiferromagnetic ordering below $T_N = 42$ K with the moment in the ab (basal) plane [12]. Single crystals of GdB_4 were synthesized by the solution growth method using Al flux, which is similar to the growth of rare earth hexaborides [13]. One of the resulting crystals was carefully cut and polished to have a flat (h 0 0) surface with the mosaicity of $\sim$0.01° at (2 0 0) for the synchrotron experiments.

Resonant x-ray scattering experiments were undertaken on the 3C2 bending magnet beam line at the Pohang Light Source (PLS) equipped with a double bounce Si(111) monochromator. A platinum coated toroidal mirror was used to focus the beam and also to eliminate higher harmonics by employing total external reflection. A prepared GdB_4 single crystal was mounted on the cold finger of a closed cycle helium displex (base temperature of $\sim$4.8 K) with azimuthal rotation configuration. The incident x-ray beam is σ polarized in the vertical scattering geometry.

First, the x-ray scattering experiments were carried out at low temperature aimed to investigate the magnetic structure of GdB_4. A Gd L_3 ($E = 7.243$ keV) absorption edge was utilized mostly for the purpose. A polarization analysis was carried out using a flat pyrolithic graphite (PG) crystal. With the PG(0 0 6) reflection, exclusive selection of the σ-to-π polarization is allowed. All the experimental results displayed were obtained for the σ-to-π-polarization channel, unless specified. Initially, the sample was aligned with the ab-(basal) plane corresponding to the scattering plane with the $[1\,0\,0] \parallel \vec{\psi}$.

Upon cooling the sample below $T_N = 42$ K, reciprocal lattice scans along the $[1\,0\,0]$ direction showed that magnetic satellite peaks emerged at $(2n + 1\,0\,0)$ position (n, integer) in addition to the fundamental $(2n\,0\,0)$ Bragg reflections. Significant enhancement of the magnetic signal was attained above the absorption edge implying that electric dipole ($E1$) transition was dominantly involved. The details of the resonance energy profile are described below along with the ATS profile.

Moreover, the azimuthal angle (ψ) dependence was obtained at (1 0 0), (3 0 0), and (5 0 0) reflections at the base temperature as shown in Fig. 1. Intensity was normalized to the fundamental (2 0 0) Bragg peak for each ψ angle to account for a possible variation in scattering volume. Intensity from multiple reflection was carefully checked and excluded when verified. Here, the azimuthal angle (ψ) is defined to be zero when the c axis lies perpendicular to the scattering plane, i.e., $\hat{c} \parallel (\vec{k}_f \times \vec{k}_i)$. Unless the magnetic structure is longitudinally modulated ($\vec{\mu} \parallel \vec{\tau}$), a sinusoidal modulation of the intensity can be anticipated from the ψ dependence due to a spin component variation in the scattering plane. Note that $I \sim (\hat{k}_f \cdot \vec{\mu})^2$ in $E1$ [7]. However, departing from simple sinusoidal oscillation, azimuthal scans in Fig. 1 exhibit remarkable phase shifts. Not only do the azimuthal scans reveal $\cos\psi$-modulation shifting from the $\psi = 0$, but also the shifted phase depends on reflection planes (Q's).

The intriguing azimuthal dependence of integrated intensity became explicable after incorporating the ATS scattering. In GdB_4, the $(2n + 1\,0\,0)$ reflections, which are forbidden by a glide plane, can be excited from the ATS. For the $E1$ transition, the resonant scattering amplitude of interest (except for a Thompson scattering) is expressed in general as

$$f_{\text{res}} \propto i(\hat{\boldsymbol{\epsilon}}_f^{\dagger} \times \hat{\boldsymbol{\epsilon}}_i) \cdot \mathbf{f}_{\text{anti}} + \hat{\boldsymbol{\epsilon}}_f^{\dagger} \cdot \mathbf{f}_{\text{sym}} \cdot \hat{\boldsymbol{\epsilon}}_i, \qquad (1)$$

where the $\hat{\boldsymbol{\epsilon}}_i$ ($\hat{\boldsymbol{\epsilon}}_f$) denotes the polarization of incident (scattered) x ray; $\mathbf{f}_{\text{anti}}$ and $\mathbf{f}_{\text{sym}}$ represent the second rank tensor of antisymmetric and symmetric traceless parts, respectively [1]. Here, the $\mathbf{f}_{\text{anti}}$ is ascribed to the magnetic and $\mathbf{f}_{\text{sym}}$ to ATS scattering [14].

ATS scattering amplitude.—The ATS scattering amplitude was constructed from a symmetric second rank tensor ($E1$) abiding by the $\mathcal{D}_{4h}$ site symmetry [6], and the geometrical scattering factor was obtained from $\mathcal{F}_{\text{ATS}}(\vec{Q}) = \sum_{j=1}^{4} e^{i\vec{Q}\cdot\vec{R}_j} \hat{\boldsymbol{\epsilon}}_f^{\dagger} \mathbf{f}_j \hat{\boldsymbol{\epsilon}}_i$, where j runs for the four Gd ions located at $\vec{R}_1{:}(x, \frac{1}{2} + x, 0)$, $\vec{R}_2{:}(\frac{1}{2} - x, x, 0)$, $\vec{R}_3{:}(-x, \frac{1}{2} - x, 0)$, and $\vec{R}_4{:}(\frac{1}{2} + x, -x, 0)$. The resulting scattering factor for the $(2n + 1\,0\,0)$ reflections is obtained for the σ-to-π polarization channel as

$$\mathcal{F}_{\text{ATS}}^{(2n+1\,0\,0)} = \mathcal{A} \cos(2\theta/2) \cos[2\pi(2n + 1)x] \sin\psi.$$

Energy dependence of the ATS strength is contained in $\mathcal{A}$. Still, the σ-to-σ channel remains forbidden in the $E1$ transition.

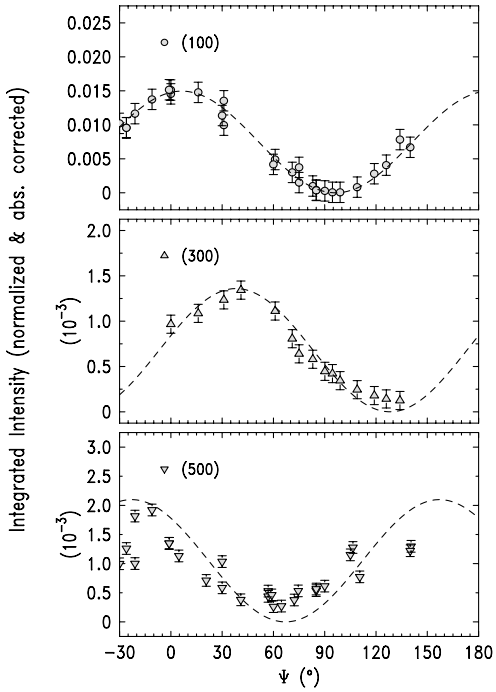

FIG. 1. Azimuthal rotation dependence of the integrated intensities ($T = 5$ K, $E = 7.246$ keV, energy of the maximum magnetic resonance) after a Lorentz factor and angle dependence of the scattering volume are corrected. The ab (basal) plane is defined as a scattering plane at $\psi = 0°$. Broken lines are obtained by considering the interference with the ATS.

Magnetic scattering amplitude.—Also, the magnetic scattering amplitude was constructed considering a transverse spin modulation [15]. A stable configuration of magnetic moments saving the bilinear exchange energy with a RKKY-type interaction was found for $\vec{\mu}_1 = \vec{\mu}_2$ and $\vec{\mu}_3 = \vec{\mu}_4 = -\vec{\mu}_1$, which is consistent with the commonly observed spin arrangement of other family compounds [16,17]. From this, the magnetic scattering amplitude was obtained from the antisymmetric term of Eq. (1) as

$$\mathcal{F}_{\text{Mag.}}^{(2n+1\,0\,0)} = \mathcal{M} \cos(2\theta/2) \sin[2\pi(2n + 1)x] \cos\psi,$$

for the σ-to-π polarization. Note that, $\mathcal{M}$ is proportional to the actual induced magnetic moment, μ.

Consequently, the total scattering amplitude from a coherent interference of simultaneously excited forbidden reflections at $(2n + 1\,0\,0)$ leads to

$$\mathcal{F}_{\text{tot}}^{(2n+1\,0\,0)} = [\mathcal{A}, \mathcal{M}]\cos(2\theta/2)\cos[\psi - \Delta(Q, \xi)],$$

$$\tan\Delta = \frac{\{\mathcal{A}, \mathcal{M}\}}{[\mathcal{A}, \mathcal{M}]}\cot[2\pi(2n+1)x],$$

where $[\alpha, \beta]$ gives α for $|\alpha| \geq |\beta|$, and conversely for the $\{\alpha, \beta\}$. Consistent with the observation, the phase shift, Δ, depends on reflection planes (Q) through $\cot[2\pi(2n+1)x]$. Its dependence on the ratio, ξ, of the interaction strength between magnetic ($\mathcal{M}$) and ATS ($\mathcal{A}$) is also noted. The relative strength of magnetic and ATS can be manipulated with ψ rotation as well, appreciating the $\pi/2$ delay in phase between the two.

The azimuthal scans were fitted to the derived scattering amplitude and the results are shown with the broken lines in Fig. 1. Stark agreements between the observed data and the derived interference scattering amplitudes could be achieved with $\mathcal{A}/\mathcal{M} \sim 0.25$. The Gd position parameter, x, is taken from the refined value of $x = 0.317$ of the isostructural TbB_4 [16]. No scaling factor among the azimuthal scans was necessary, except for the intensity at the (1 0 0) reflection with a factor of $\sim$1.7. Considering a very small reflection angle for the (1 0 0) reflection with $\theta = 3$–$5°$, this arbitrary scaling factor could be a result of a different condition in scattering volume with the beam size comparable to the sample size. Overall, the data were well reproduced from the derived scattering amplitude.

To further convince one that the phase shift in the azimuthal dependence was a result of the interference between the magnetic and the ATS resonances, pure ATS scattering was explored at $T = 99$ K above the $T_N = 42$ K. Azimuthal scans were repeated for $(2n + 1\,0\,0)$ reflections at $T = 99$ K. Now, without any interference with the magnetic reflections, the azimuthal rotation was expected to be in phase irrespective of the reflection planes with the maximum intensity at $\psi = 90°$. Figure 2 shows the azimuthal scans of the (1 0 0) and (3 0 0) forbidden reflections. Indeed, consistent with the pure ATS scattering amplitude, modulations are found in phase for

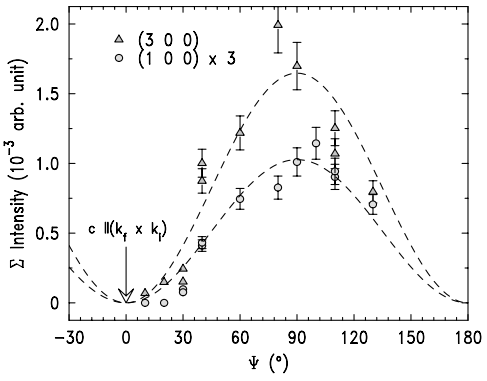

FIG. 2. Azimuthal scans of the pure ATS reflections ($E = 7.249$ keV, $T = 99$ K). Without interference from magnetic scattering, the azimuthal dependence is observed in phase. Broken lines are the derived ATS scattering intensity.

different reflections and maximum intensity of the modulation is noted at $\psi = 90°$.

Next, we turn to an electronic structure of a Gd 5d band inferred from the two reflections. Figure 3 displays the various energy profiles of the magnetic ($T = 5$ K, $\psi = 0°$) (b), ATS reflections ($T = 99$ K, $\psi = 90°$) (c), along with the (2 0 0) Bragg peak intensity showing charge absorption (a) and x-ray absorption spectrum (XAS) at the boron K edge (d). This result clearly demonstrates that mode-selective energy profiles can be obtained by RXS while the normal x-ray absorption spectrum near the B K edge provides mode-integrated ones: The energy profiles of magnetic and ATS reflections of GdB_4 can be selectively probed by a judicious choice of the azimuthal angle (ψ). Most interesting to note is the marked differences in the maximum resonance energy as well as the overall energy structure between the two resonance profiles of RXS. The noted separation between the resonance energies is significant with $\sim 7(\pm 3)$ eV:7.245 (magnetic), 7.249 and 7.255 keV (ATS). Here, 7.245 keV of the magnetic resonance is the nominal value from the fit corresponding more to the resonance center rather than the actual maximum resonance of 7.246 keV.

Since the magnetic and ATS are excited via the same $E1$ transition of $2p_{3/2}$ to 5d, the energy profile is rather attributed to a structure within the Gd 5d band. Various hybridizations result in the splitting of the 5d band into the lower (7.245 keV) and upper energy states (7.249 and 7.255 keV): Intra-atomic band mixing and direct exchange coupling with the Gd 4f state lead to the lower band with magnetic sensitivity, whereas an interatomic hybridization with the nearby boron atoms (B 2p states) distorts the 5d band more severely, leading to the ATS resonances appearing at the upper 5d band. Note also that the band mixing with the spherical Gd 4f orbital ($^8S_{7/2}$) is not viable to induce anisotropic charge distribution, as indeed the case here with a relatively weak ATS signal at 7.245 keV.

The boron K-edge XAS, which is shifted by the energy difference between the B K-edge and Gd L_3-edge absorption energies to be aligned with the absorption threshold, was compared in Fig. 3 to support our interpretation given above. The XAS measurement was performed on the 8 A beam line of PLS. The spectrum was obtained from a clean surface by scraping with a diamond file *in situ*, and the photon energy resolution was set to be about 0.1 eV. The B K-edge XAS reflects the Gd 4f and 5d bands due to the hybridization with the B 2p states. The spectrum indeed displays an ample distribution of Gd 5d states shifted upward due to the strong bonding with the B 2p states. Furthermore, observed ATS resonances, including the fine structure with two maxima, coincide well with the structure in XAS explicitly evidencing that distortion of the valence charge distribution was reinforced by hybridization with B 2p orbitals to drive the ATS. The Gd 4f state shows relatively weak absorption intensity around $\sim$4 eV above the threshold energy implying weak

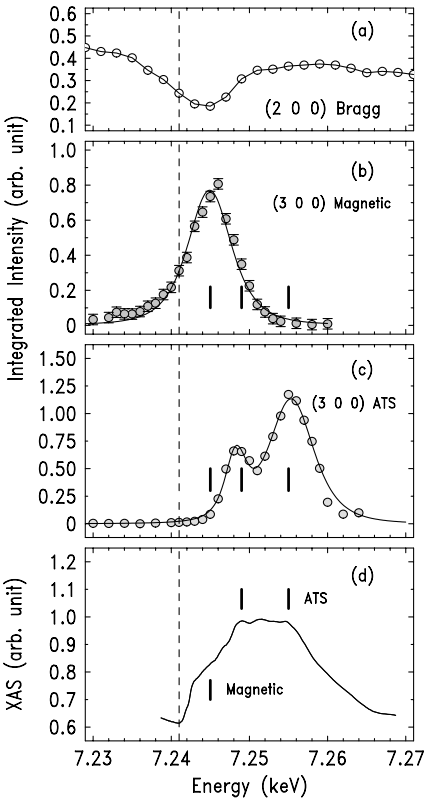

FIG. 3. Energy profiles near the Gd L_3 edge. (a) X-ray scattering intensity at the (2 0 0) Bragg peak. (b) Resonance energy profile of the (3 0 0) magnetic peak taken at $T = 5$ K and $\psi = 0°$. (c) Resonance profile from ATS ($T = 99$ K and $\psi = 90°$). (d) X-ray absorption spectrum emphasizing the boron $2p$ states after shifting the Fermi level to the absorption edges in (a)–(c) for a comparison on the same energy scale. Solid bars denote the maximum resonance energies of magnetic and ATS. Broken vertical lines denote the absorption edge determined from the maximum derivative of (2 0 0) charge peak's absorption profile. Intensities of magnetic (b) and ATS (c) were scaled by multiplying 10^5, and no absorption correction was considered. Energy profiles in (b) and (c) were fitted to empirical Lorentzian squared line shapes mainly used to guide the eye.

hybridization with the B $2p$ states. A more detailed understanding on the fine structure of the ATS resonance would require refined theoretical model analysis for the resonant x-ray scattering, which is beyond the scope of this paper.

In summary, we present the first direct evidence of coherent interference between simultaneously excited magnetic and ATS resonances in GdB_4 causing appreciable phase shifts in the azimuthal dependence. Resonance energy profiles of the magnetic and ATS reflections were separated by rotating the azimuthal (ψ) angle. Through the resonance energy profiles, hybridization of Gd $5d$ orbitals was revealed. The spin polarization and anisotropic charge distribution were realized on different portions of the split $5d$ bands. Implications of the current work are profound. Most of all, this work demonstrated that various physical characters of the electronic states can be probed by exploiting the rich resonance energy spectra of the RXS. Especially, RXS can be utilized as a spectroscopy probe which enables selective investigation of electronic states relevant to the magnetic interactions and anisotropic charge distributions whose interplay is the keen interest in strongly correlated electron systems.

The authors have benefitted from stimulating discussions with C. Detlefs, especially on the ATS. This work is supported by the BK-21 Program and the KOSEF through the electron Spin Science Center at POSTECH, and by KISTEP through the X-ray/particle-beam Nanocharacterization Program. The experiment at the Pohang Light Source is supported by the POSTECH Foundation and MOST. The work at K-JIST is supported by CSCMR at SNU funded by KOSEF. One of us (J. H. P.) is also supported by KRF (2002-070-C00038).

[1] M. Blume, in *Resonant Anomalous X-ray Scattering*, edited by G. Materlik, C. J. Spark, and K. Fisher (North-Holland, Amsterdam, 1994), pp. 495–515.
[2] D. Gibbs *et al.*, Phys. Rev. Lett. **61**, 1241 (1988).
[3] K. Namikawa, M. Ando, T. Nakajima, and H. Kawata, J. Phys. Soc. Jpn. **54**, 4099 (1985).
[4] J. P. Hannon, G. T. Trammel, M. Blume, and D. Gibbs, Phys. Rev. Lett. **61**, 1245 (1998).
[5] D. H. Templeton and L. K. Templeton, Acta Crystallogr. Sect. A **38**, 62 (1982).
[6] V. E. Dmitrienko, Acta Crystallogr. Sect. A **39**, 29 (1983).
[7] J. P. Hill, in *Characterization of Materials*, edited by E. N. Kaufmann (Wiley, New York, 2003), pp. 917–939, and references therein.
[8] Y. Murakami *et al.*, Phys. Rev. Lett. **80**, 1932 (1998); Y. Murakami *et al.*, Phys. Rev. Lett. **81**, 582 (1998).
[9] L. Paolasini *et al.*, Phys. Rev. Lett., **82**, 4719 (1999).
[10] K. D. Finkelstein, Q. Shen, and S. Shastri, Phys. Rev. Lett. **69**, 1612 (1993).
[11] E. N. Ovchinnikova and V. E. Dmitrienko, Acta Crystallogr. Sect. A **53**, 388 (1997); **56**, 2 (2000).
[12] Z. Fisk, M. B. Maple, D. C. Johnston, and L. D.Woolf, Solid State Commun. **39**, 1189 (1981).
[13] J. S. Rhyee, C. A. Kim, B. K. Cho, and H. C. Ri, Phys. Rev. B **65**, 205112 (2002).
[14] The magnetic term also leads to the $\mathbf{f}_{\mathrm{sym}}$ via μ^2, but with the spin modulation at the zone boundary the μ^2 satellites appear at the zone center along with intense Bragg reflections, which is not of current concern.
[15] Contribution from a longitudinal component of the moment, if any, may result in a constant shift of the intensity without altering major interference behavior.
[16] F. Elf, W. Schäfer, G. Will, and J. Etourneou, Solid State Commun. **40**, 579 (1981).
[17] W. Schäfer, G. Will, and K. H. J. Buschow, J. Chem. Phys. **64**, 1994 (1976).